COMPDYN 2015
5th ECCOMAS Thematic Conference on
Computational Methods in Structural Dynamics and Earthquake Engineering
M. Papadrakakis, V. Papadopoulos, V. Plevris (eds.)
Crete Island, Greece, 25–27 May 2015

GENERALIZED WARPING EFFECT IN THE DYNAMIC ANALYSIS OF BEAMS OF ARBITRARY CROSS SECTION

Ioannis C. Dikaros[1], **Evangelos J. Sapountzakis**[2], **Amalia K. Argyridi**[3] **and Dimitris S. Papadopoulos**[4]

[1]School of Civil Engineering, National Technical University of Athens
Zografou Campus, GR–157 80, Athens, Greece
dikarosgiannis@gmail.com.

[2-3]School of Civil Engineering, National Technical University of Athens
Zografou Campus, GR–157 80, Athens, Greece
cvsapoun@central.ntua.gr, a.argyridi@gmail.com.

[4]Engineer Officers Technical School, Corps of Engineers, Hellenic Army General Staff
Papadiamantopoulou 190, GR-115 27, Athens, Greece,
papadopoulosdimitris9@gmail.com.

Keywords: Nonuniform warping; Shear lag; Shear deformation; Dynamic Analysis; Boundary Element Method.

Abstract. *In this paper a general formulation for the nonuniform warping dynamic analysis of beams of arbitrary simply or multiply connected cross section, under arbitrary external loading and general boundary conditions is presented taking into account the effects of rotary and warping inertia. The nonuniform warping distributions are taken into account by employing four independent warping parameters multiplying a shear warping function in each direction and two torsional warping functions, respectively, which are obtained by solving the corresponding boundary value problems, formulated exploiting the longitudinal local equilibrium equation. A shear stress "correction" is also performed in order to improve the stress field arising from the employed kinematical considerations. Ten initial boundary value problems are formulated with respect to the displacement and rotation components as well as to the independent warping parameters and solved using the Analog Equation Method, a Boundary Element Method based technique in combination with an appropriate time integration scheme. The warping functions and the geometric constants including the additional ones due to warping are evaluated employing a pure BEM approach.*

1 INTRODUCTION

In engineering practice, the dynamic analysis of beam-like members under flexure is frequently encountered. Besides, many conditions occurring in engineering practice, such as rotating machinery, wind and traffic loads, blast and earthquake forces, require taking into account inertial effects in the dynamic analysis of beams. The inclusion of such effects, especially through distributed mass models, which are considered to be more reliable, requires a rigorous analysis. In the vast majority of these cases, Euler – Bernoulli beam theory assumptions are adopted, and when shear deformation effect is non-negligible these assumptions are relaxed by using Timoshenko beam theory. However, both theories maintain the assumption that plane cross sections remain plane after deformation. By maintaining this assumption, the formulation remains simple; however, it fails to capture the well-known shear lag phenomenon, which was reported long ago (e.g. [1-3]) and observed in many structural members (e.g., beams of box-shaped cross sections, folded structural members, beams made of materials weak in shear). Shear lag is associated with a significant modification of normal stress distribution, especially near the joint of the various cross-sectional components [4], due to nonuniform distribution of shear warping [Figs. 1(d and e)] [5].

In up-to-date regulations, the significance of shear lag effect in flexure is recognized; however, to simplify the analysis, the effective width concept [6-8] is recommended. This simplifying approach may fail to capture satisfactorily the actual structural behaviour of the member, because the influence of the shear lag phenomenon is not constant along the beam length. Apart from the geometrical configuration of the cross section, it depends also on the type of loading [9]. Therefore, it is necessary to include the effects of nonuniform shear warping distribution in both the static and the dynamic analysis.

Generalizing the shear lag analysis problem, considerations similar to those made for flexure could be also adopted for the problem of torsion. It is well known that when a beam undergoes general twisting loading under general boundary conditions, it is led to nonuniform torsion. This problem has been extensively examined in the literature (e.g. see [10,11]), and its major characteristic is the presence of normal stress due to primary torsional warping [Fig. 1(c)]. In an analogy with Timoshenko beam theory, when shear deformation is of importance, the so-called secondary torsional shear deformation effect (STSDE) [12,13] has to be taken into account as well. Thus, it could be concluded that the additional secondary torsional warping due to STSDE [Fig. 1(f)] can cause effects similar to shear lag in flexure, i.e., a modification of the initial normal stress distribution. It is noted that because of the complicated nature of torsion, simplified concepts such as effective width cannot be applied to take this behavior into account.

Toward investigating shear lag effects, the inclusion of nonuniform warping in beam element formulations based on so-called higher-order beam theories [14] is of increased interest because of their important advantages over more refined approaches (e.g. [15-17]). Beam elements are practical and computationally efficient and offer better insight into the structural phenomena, since they permit their isolation and independent investigation. Furthermore, because of easy parameterization of all necessary data, beam elements are more convenient for parametric analyses than more refined models which, in most cases, require the construction of multiple models.

The dynamic analysis of the generalized nonuniform warping problem has received relatively less attention than the static one. Some researchers have employed the assumptions of TTT (Thin Tube Theory) and the nonuniform torsion theory with an additional degree of freedom for nonuniform warping that is the rate of angle of twist [23-34] or an independent

warping parameter [35-36]. Egidio et al [37] describe the non-linear warping of open cross-section thin-walled beams in terms of the flexural and torsional curvatures. Minghini et al [38] take into account shear strain effects due to both nonuniform bending and torsion in the analysis of thin walled cross sections. Some other researchers have employed the nonuniform torsion theory for beams with arbitrarily shaped cross sections with the rate of the angle of twist as an additional degree of freedom [39-46].Sapountzakis and Tsipiras [47] have taken into account nonouniform torsion in the analysis of beam with arbitrarily shaped doubly symmetric cross sections using a secondary warping function. On the other hand Li et al [48] developed an element that includes the effect of warping using a displacement field that is assumed to be cubic in the axial direction and quadratic in the transverse direction. Moreover, to the authors ' knowledge, a BEM procedure for the dynamic analysis of the general nonuniform warping problem of beams of arbitrary cross sections has never been reported in the literature.

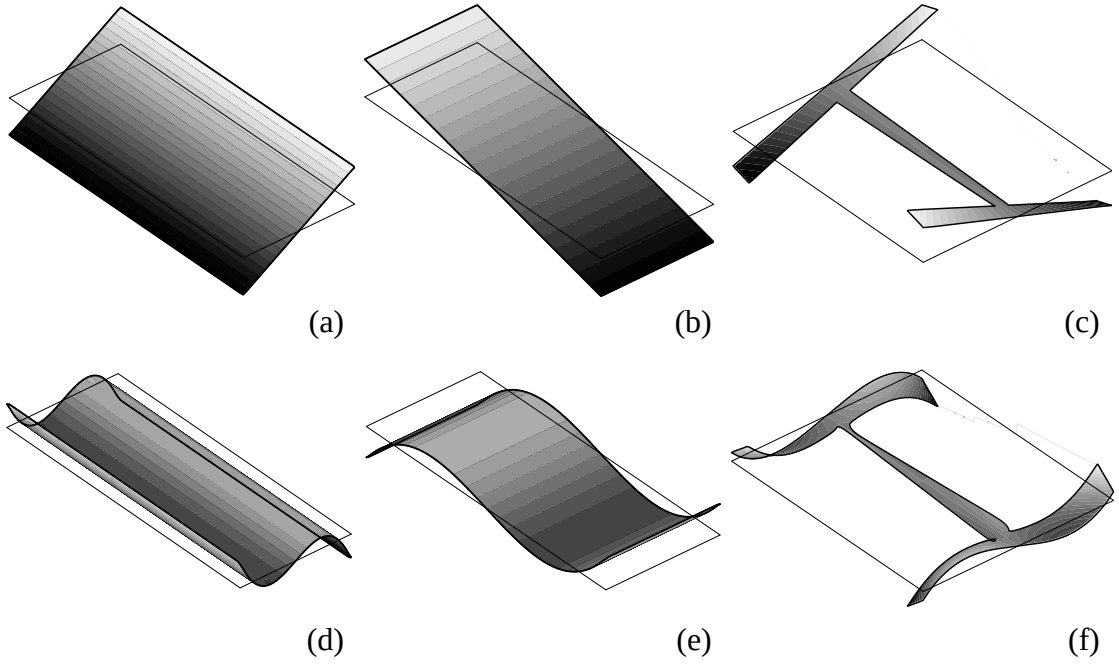

Fig.1. Normal stress distribution due to flexure (a,b), primary torsional warping (c), shear warping (d,e) and secondary torsional warping (f).

In the current study, which is an extension of a previous work of the same authors [49-50] at the dynamic regime, a general boundary element formulation for the dynamic nonuniform warping analysis of beams of arbitrary cross section, taking into account shear lag effects due to both flexure and torsion, is presented. The beam cross section (thin- or thick-walled) is homogeneous and can surround a finite number of inclusions. The beam is subjected to the combined action of arbitrarily distributed or concentrated dynamic axial loading and transverse loading, as well as to bending, twisting, and warping moments. Nonuniform warping distributions are taken into account by using four independent warping parameters multiplying a shear warping function in each direction [49-50] and two torsional warping functions, which are obtained by solving corresponding boundary value problems. It is worth mentioning here that the stress field arising from the preceding kinematical considerations leads to the violation of the longitudinal local equilibrium equation and the corresponding boundary condition [22] due to inaccurate representation of shear stresses. In the current study, to keep the sim-

plicity of the formulation to the highest possible level, the increment of the number of unknowns in global equilibrium is avoided and a correction of the stress field is performed with the aid of the longitudinal local equilibrium equation. Ten initial-boundary value problems are formulated with respect to the displacement and rotation components and the independent warping parameters and solved using the analog equation method (AEM) [52], a BEM-based method in combination with an appropriate time integration scheme (Mean Acceleration Method [56]). The warping functions, the additional geometric constants due to warping, and the elementary ones are evaluated with a pure BEM approach, i.e., only boundary discretization of the cross section is used. After establishment of the kinematical components, the aforementioned boundary discretization can be used to evaluate through BEM the normal and shear stress components at any arbitrary point of each cross section.

The essential features and novel aspects of the present formulation are summarized as follows:

- The cross section is an arbitrarily shaped thin- or thick-walled. The formulation does not stand on the assumption of a thin-walled structure, and therefore the cross section's warping rigidities are evaluated exactly (in a numerical sense).
- An improved stress field is adopted with the aid of the longitudinal local equilibrium equation, leading to a better evaluation of stress components without increasing the global degrees of freedom.
- The beam is subjected to arbitrary external loading and is supported by the most general boundary conditions, including elastic support or restraint.
- The proposed formulation is suitable for the investigation of flexural and torsional shear lag effects in beams of closed or open cross sections.
- The proposed method uses a BEM approach (requiring boundary discretization for the cross-sectional analysis) resulting in line or parabolic elements instead of area elements of the FEM solutions (requiring the whole cross section to be discretized into triangular or quadrilateral area elements), whereas a small number of line elements are required to achieve high accuracy.
- The use of BEM permits the accurate computation of deriveatives of the field functions (e.g., stresses) which is very important in the nonuniform warping analysis of beams.
- The generalized warping theory of beams presented in [49-50] is extended at the dynamic regime.
- The necessity to include warping inertial and generalized warping effects is investigated in both thin- and thick walled open- and closed shaped cross section bars.
- Both free and forced vibrations of bars are investigated obtaining free vibration characteristics and both kinematic and stress results in the time domain, respectively.

2 STATEMENT OF THE PROBLEM

2.1 Displacement, strain and stress components

Consider a prismatic beam of length l, of arbitrary cross section of area A. The homogeneous isotropic and linearly elastic material of the beam's cross section, with modulus of elasticity E, shear modulus G, Poisson's ratio ν and mass density ρ occupies the two dimensional multiply connected region Ω of the yz plane and is bounded by the Γ_j ($j=1,2,...,K$) boundary curves, which are piecewise smooth, i.e. they may have a finite number of corners. In Fig.2 $CXYZ$ is the principal bending coordinate system through the cross section's centroid C, while y_C, z_C are its coordinates with respect to $Sxyz$ reference system of axes through

the cross section's center of twist S. The beam is subjected to the combined action of the arbitrarily distributed or concentrated time-dependent axial loading $p_x = p_x(X,t)$ along X direction, transverse loading $p_y = p_y(x,t)$, $p_z = p_z(x,t)$ along the y, z directions, respectively, twisting moments $m_t = m_t(x,t)$ along x direction, bending moments $m_Y = m_Y(x,t)$, $m_Z = m_Z(x,t)$ along Y, Z directions, respectively, as well as warping moments $m_{\varphi_S^P} = m_{\varphi_S^P}(x,t)$, $m_{\varphi_S^S} = m_{\varphi_S^S}(x,t)$, $m_{\varphi_{CY}^P} = m_{\varphi_{CY}^P}(x,t)$, $m_{\varphi_{CZ}^P} = m_{\varphi_{CZ}^P}(x,t)$ (Fig.2) which will be later defined in section 2.2.

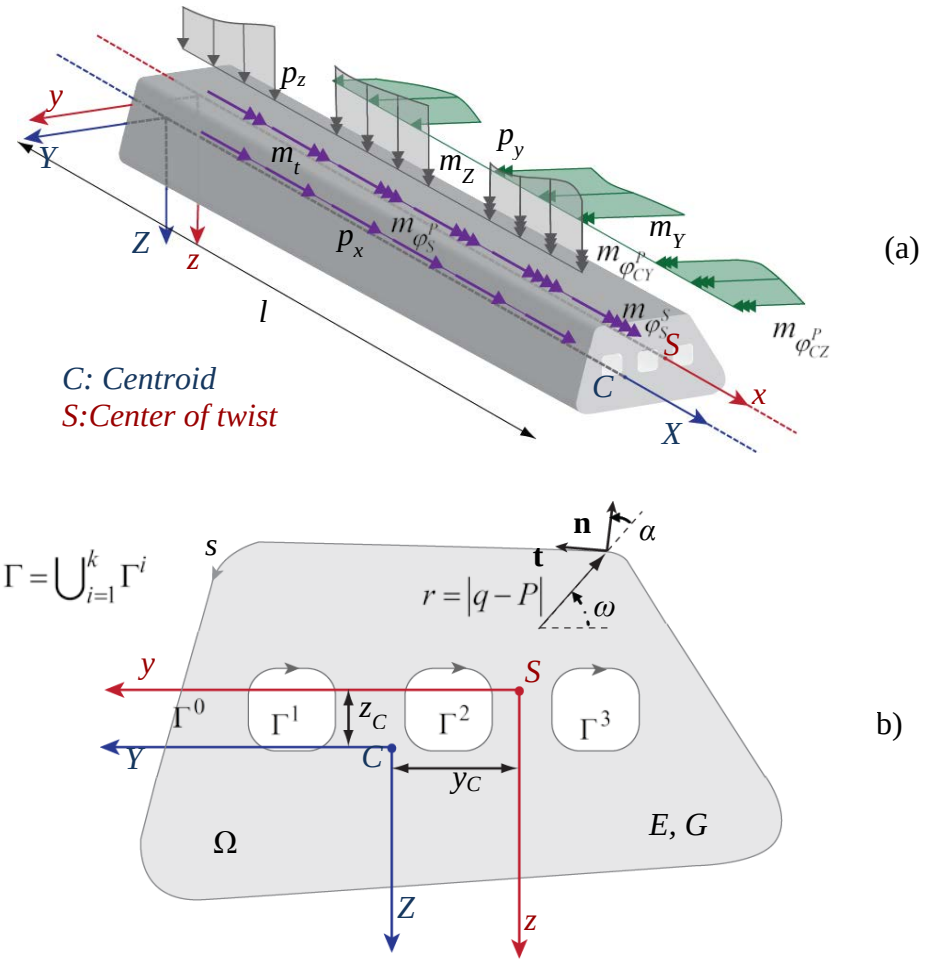

Fig.2. Prismatic beam under axial-flexural-torsional dynamic loading (a) of an arbitrary cross section occupying the two dimensional region Ω (b).

Under the action of the aforementioned general loading and of possible restraints, the beam is leaded to flexural, axial and/or torsional vibrations. In order to take into account nonuniform warping distributions which are responsible for shear lag effects due to both flexure and torsion, four additional time-dependent degrees of freedom (warping parameters), namely $\eta_x(x,t)$, $\eta_Y(x,t)$, $\eta_Z(x,t)$, $\xi_x(x,t)$ multiplying a shear warping function in each direction (η_Y, η_Z) and two torsional warping functions (η_x, ξ_x), respectively, are employed [49, 50]. These additional DOFs describe the "intensities" of the corresponding cross sectional warping along the beam length at any time instant, while these warpings are defined by corresponding

warping functions ($\varphi_{CY}^{P}(y,z)$, $\varphi_{CZ}^{P}(y,z)$, $\varphi_{S}^{P}(y,z)$, $\varphi_{S}^{S}(y,z)$), depending only on the cross sectional configuration. Thus, the "actual" deformed configurations of the cross section due to primary (in each direction) shear and primary, secondary torsional warpings are given as $\eta_Y(x,t)\varphi_{CY}^{P}(y,z)$, $\eta_Z(x,t)\varphi_{CZ}^{P}(y,z)$, $\eta_x(x,t)\varphi_{S}^{P}(y,z)$ and $\xi_x(x,t)\varphi_{S}^{S}(y,z)$ at any position and time instant. It is worth here noting that the shear stresses generated by the above displacement considerations exhibit an inconsistency concerning the non-vanishing of tractions τ_{xn} on the lateral surface of the beam [22, 49, 50]. As shown in previous studies, this inconsistency may be responsible for non-negligible errors in estimated normal stress values. In the present study this inconsistency is removed by performing a suitable shear stress correction, which is discussed in detail in a previous work of the same authors [49, 50]. Within the context of the above considerations, the displacement components of an arbitrary point of the beam at an arbitrary time instant are given as

$$\begin{aligned}\bar{u}(x,y,z,t) &= \bar{u}^{P}(x,y,z,t)+\bar{u}^{S}(x,y,z,t)= \\ &= \underbrace{u(x,t)+\theta_Y(x,t)Z-\theta_Z(x,t)Y+\eta_x(x,t)\phi_{S}^{P}(y,z)}_{\text{primary}}+ \\ &+\underbrace{\eta_Y(x,t)\phi_{CY}^{P}(y,z)+\eta_Z(x,t)\phi_{CZ}^{P}(y,z)+\xi_x(x,t)\phi_{S}^{S}(y,z)}_{\text{secondary}}\end{aligned} \tag{1a}$$

$$\bar{v}(x,y,z,t)=v(x,t)-z\theta_x(x,t) \qquad \bar{w}(x,y,z,t)=w(x,t)+y\theta_x(x,t) \tag{1b,c}$$

where $\bar{u}$, $\bar{v}$, $\bar{w}$ are the axial and transverse beam displacement components with respect to the $Sxyz$ system of axes, while $\bar{u}^{P}$, $\bar{u}^{S}$ denote the primary and secondary longitudinal displacements, respectively. Moreover, $v(x,t)$, $w(x,t)$ describe the deflection of the center of twist S, while $u(x,t)$ denotes the "average" axial displacement of the cross section. $\theta_Z(x,t)$, $\theta_Y(x,t)$ are the angles of rotation due to bending about the centroidal Y, Z axes, respectively. $\eta_x(x,t)$, $\xi_x(x,t)$ are the independent warping parameters introduced to describe the nonuniform distribution of primary and secondary torsional warping, while $\eta_Y(x,t)$, $\eta_Z(x,t)$ are the independent warping parameters introduced to describe the nonuniform distribution of primary warping due to shear [49, 50]. $\varphi_{S}^{P}(y,z)$, $\varphi_{S}^{S}(y,z)$ are the primary and secondary torsional warping functions with respect to the center of twist S [13], while $\varphi_{CY}^{P}(y,z)$, $\varphi_{CZ}^{P}(y,z)$ are the primary shear warping functions with respect to the centroid C [49, 50]. Finally, it holds that $Z=z-z_C$, $Y=y-y_C$.

Employing the displacement expressions given from eqns. (1) to the strain-displacement relations of the three-dimensional elasticity for small displacements and the Hooke's stress-strain law, the non-vanishing components of the Cauchy stress tensor are obtained as

$$\sigma_{xx}=\underbrace{E^{*}\left[u_{,x}+\theta_{Y,x}Z-\theta_{Z,x}Y+\eta_{x,x}\varphi_{S}^{P}\right]}_{\text{primary}}+\underbrace{E^{*}\left[\eta_{Y,x}\varphi_{CY}^{P}+\eta_{Z,x}\varphi_{CZ}^{P}+\xi_{x,x}\varphi_{S}^{S}\right]}_{\text{secondary}} \tag{2a}$$

$$\mathbf{t} = \underbrace{G\left[\gamma_Z^P \nabla\left(Z+\varphi_{CY}^P\right)+\gamma_Y^P \nabla\left(Y+\varphi_{CZ}^P\right)+\gamma_x^P\left(\mathbf{r}+\nabla\varphi_S^P\right)\right]}_{\text{primary}}+$$
$$+\underbrace{G\left[\gamma_Z^S \nabla\varphi_{CY}^S+\gamma_Y^S \nabla\varphi_{CZ}^S+\gamma_x^S \nabla\left(\varphi_S^P+\varphi_S^S\right)\right]}_{\text{secondary}}+\underbrace{G\left[\gamma_x^T \nabla\varphi_S^S\right]}_{\text{tertiary}} \tag{2b}$$

where $\mathbf{t}=\left[\tau_{xy} \quad \tau_{xz}\right]^T$, $\mathbf{r}=\left[-z \quad y\right]^T$ and $E^* = E(1-\nu)/\left[(1+\nu)(1-2\nu)\right]$. If the plane stress hypothesis is undertaken then $E^* = E/\left(1-\nu^2\right)$ holds [10], while E is frequently considered instead of E^* ($E^* \approx E$) in beam formulations [10]. The first consideration has been followed throughout the paper, while any other reasonable expression of E could also be used without any difficulty. Furthermore, $(\cdot)_{,i}$ denotes differentiation with respect to i, while $\nabla \equiv (\cdot)_{,y}\,\mathbf{i}_y + (\cdot)_{,z}\,\mathbf{i}_z$ is the gradient operator and $\mathbf{i}_y$, $\mathbf{i}_z$ the unit vectors along y, z axes, respectively. $\gamma_x^P = \theta_{x,x}$, $\gamma_x^S = \eta_x - \theta_{x,x}$, $\gamma_x^T = \xi_x - \eta_x + \theta_{x,x}$, $\gamma_Y^P = v_{,x} - \theta_Z$, $\gamma_Y^S = \eta_Y - v_{,x} + \theta_Z$, $\gamma_Z^P = w_{,x} + \theta_Y$ and $\gamma_Z^S = \eta_Z - w_{,x} - \theta_Y$ are "average" shear strain quantities. In eqns. (2b) the primary shear stress terms correspond to the St. Venant shear stresses (τ_{xy}^P, τ_{xz}^P) [14], while the rest of the terms to warping shear stresses (τ_{xy}^S, τ_{xz}^S, τ_{xy}^T, τ_{xz}^T) arising from the use of independent warping parameters. The above stress components (2) could be employed in order to derive the global equations of motion. However, as stated above, attention should be paid to the fact that the terms $\gamma_Y^S \varphi_{CY,i}^P$, $\gamma_Z^S \varphi_{CZ,i}^P$, $\gamma_x^T \varphi_{S,i}^S$ ($i = y, z$) are not capable of representing an acceptable shear stress distribution, leading to violation of the longitudinal local equilibrium equation and the corresponding zero-traction condition on the lateral surface of the beam. This observation reveals an analogy with Timoshenko beam theory and nonuniform torsion theory with STSDE [12,13]. As a consequence, discrepancies in stress components near fixed supports or concentrated loads may arise [12,13,21,49,50]. In the present study, a correction of stress components is performed without increasing the number of global kinematical unknowns, following the analysis presented in [49, 50]. To this end, three additional warping functions $\varphi_{CY}^S(y,z)$, $\varphi_{CZ}^S(y,z)$, $\varphi_S^T(y,z)$ are introduced in expressions (2b), which are modified as

$$\mathbf{t} = \underbrace{G\left[\gamma_Z^P \nabla\Phi_{CY}^P+\gamma_Y^P \nabla\Phi_{CZ}^P+\gamma_x^P\left(\mathbf{r}+\nabla\varphi_S^P\right)\right]}_{\text{primary}}+\underbrace{G\left[\gamma_Z^S \nabla\Phi_{CY}^S+\gamma_Y^S \nabla\Phi_{CZ}^S+\gamma_x^S \nabla\Phi_S^S\right]}_{\text{secondary}}+$$
$$+\underbrace{G\left[\gamma_x^T \nabla\Phi_S^{\mathrm{T}}\right]}_{\text{tertiary}} \tag{3}$$

where

$$\Phi_{CY}^P = Z + \varphi_{CY}^P \qquad \Phi_{CY}^S = \varphi_{CY}^P + \varphi_{CY}^S \tag{4a,b}$$
$$\Phi_{CZ}^P = Y + \varphi_{CZ}^P \qquad \Phi_{CZ}^S = \varphi_{CZ}^P + \varphi_{CZ}^S \tag{4c,d}$$

$$\Phi_S^S = \varphi_S^P + \varphi_S^S \qquad \Phi_S^T = \varphi_S^S + \varphi_S^T \tag{4e,f}$$

Warping functions (4) can be determined by formulating boundary value problems exploiting the longitudinal local equilibrium equation and the associated boundary condition, which will be discussed in next section.

2.2 Global equations of motion

In order to establish the differential equations of motion, the principle of virtual work including virtual work due to inertial forces

$$\delta W_{\text{int}} + \delta W_{\text{mass}} = \delta W_{\text{ext}} \tag{5}$$

is employed, where

$$\delta W_{\text{int}} = \int_V \left(\sigma_{xx}\delta\varepsilon_{xx} + \tau_{xy}\delta\gamma_{xy} + \tau_{xz}\delta\gamma_{xz} \right) \mathrm{d}V \tag{6a}$$

$$\delta W_{\text{mass}} = \int_V \rho \left(\overline{u}_{,tt}\delta\overline{u} + \overline{v}_{,tt}\delta\overline{v} + \overline{w}_{,tt}\delta\overline{w} \right) \mathrm{d}V \tag{6b}$$

$$\delta W_{\text{ext}} = \int_{\text{Lat}} \left(t_x\delta\overline{u} + t_y\delta\overline{v} + t_z\delta\overline{w} \right) \mathrm{d}F \tag{6c}$$

In the above equations, $\delta(\cdot)$ denotes virtual quantities; t_x, t_y, t_z are the components of the traction vector applied on the lateral surface of the beam including the end cross sections, denoted by F and V is the volume of the beam. Moreover, the stress resultants of the beam can be defined as

$$N = \int_\Omega \sigma_{xx}\,\mathrm{d}\Omega \qquad M_Y = \int_\Omega \sigma_{xx} Z\,\mathrm{d}\Omega \qquad M_Z = \int_\Omega \sigma_{xx} Y\,\mathrm{d}\Omega \tag{7a,b,c}$$

$$M_{\varphi_S^P} = \int_\Omega \sigma_{xx}\varphi_S^P\,\mathrm{d}\Omega \qquad M_{\varphi_S^S} = \int_\Omega \sigma_{xx}\varphi_S^S\,\mathrm{d}\Omega \tag{7d,e}$$

$$M_{\varphi_{CY}^P} = \int_\Omega \sigma_{xx}\varphi_{CY}^P\,\mathrm{d}\Omega \qquad M_{\varphi_{CZ}^P} = \int_\Omega \sigma_{xx}\varphi_{CZ}^P\,\mathrm{d}\Omega \tag{7f,g}$$

$$Q_y^P = \int_\Omega \left(\tau_{xy}\Phi_{CY,y}^P + \tau_{xz}\Phi_{CY,z}^P \right) \mathrm{d}\Omega \qquad Q_y^S = -\int_\Omega \left(\tau_{xy}\Phi_{CY,y}^S + \tau_{xz}\Phi_{CY,z}^S \right) \mathrm{d}\Omega \tag{7h,i}$$

$$Q_z^P = \int_\Omega \left(\tau_{xy}\Phi_{CZ,y}^P + \tau_{xz}\Phi_{CZ,z}^P \right) \mathrm{d}\Omega \qquad Q_z^S = -\int_\Omega \left(\tau_{xy}\Phi_{CZ,y}^S + \tau_{xz}\Phi_{CZ,z}^S \right) \mathrm{d}\Omega \tag{7j,k}$$

$$M_t^P = \int_\Omega \left[\tau_{xy}\left(\varphi_{S,y}^P - z \right) + \tau_{xz}\left(\varphi_{S,z}^P + y \right) \right] \mathrm{d}\Omega \tag{7l,m}$$

$$M_t^S = -\int_\Omega \left(\tau_{xy}\Phi_{S,y}^S + \tau_{xz}\Phi_{S,z}^S \right) \mathrm{d}\Omega \qquad M_t^T = \int_\Omega \left(\tau_{xy}\Phi_{S,y}^T + \tau_{xz}\Phi_{S,z}^T \right) \mathrm{d}\Omega \tag{7n,o}$$

where M_i ($i = Y, Z$) are the bending moments and M_i ($i = \varphi_S^P, \varphi_S^S, \varphi_{CY}^P, \varphi_{CZ}^P$) are the warping moments (bimoments). Q_i^j ($i = y, z$ $j = P, S$) are the primary and secondary parts of total shear forces Q_i ($i = y, z$). It is noted that the secondary shear forces are also referred to as bishear stress resultants [5,18] since they equilibrate the corresponding warping moments (bimoments). Similarly, M_t^j ($j = P, S, T$) are the primary, secondary and tertiary parts of total twisting moment M_t. Moreover, the geometric constants of the beam can be obtained by the following definitions [49, 50]

$$A=\int_{\Omega}\mathrm{d}\Omega \qquad S_Y=\int_{\Omega}Z\,\mathrm{d}\Omega \qquad S_Z=\int_{\Omega}Y\,\mathrm{d}\Omega \tag{8a-c}$$

$$I_{YY}=\int_{\Omega}Z^2\,\mathrm{d}\Omega \qquad I_{ZZ}=\int_{\Omega}Y^2\,\mathrm{d}\Omega \qquad I_{YZ}=\int_{\Omega}YZ\,\mathrm{d}\Omega \tag{8d-f}$$

$$S_i=\int_{\Omega}(i)\,\mathrm{d}\Omega,\quad i=\varphi_S^P,\varphi_S^S,\varphi_{CY}^P,\varphi_{CZ}^P \tag{8g}$$

$$I_{ij}=\int_{\Omega}(i)(j)\,\mathrm{d}\Omega,\quad i,j=y,z,\varphi_S^P,\varphi_S^S,\varphi_{CY}^P,\varphi_{CZ}^P \tag{8h}$$

$$D_{ij}=\int_{\Omega}\nabla(i)\cdot\nabla(j)\,\mathrm{d}\Omega,\quad i,j=\Phi_S^S,\Phi_S^{\mathrm{T}},\Phi_{CY}^P,\Phi_{CY}^S,\Phi_{CZ}^P,\Phi_{CZ}^S \tag{8i}$$

$$I_t^P=\int_{\Omega}\left(y^2+z^2-z\varphi_{S,y}^P+y\varphi_{S,z}^P\right)\mathrm{d}\Omega \tag{8j}$$

$$I_p=\int_{\Omega}\left(y^2+z^2\right)\mathrm{d}\Omega \tag{8k}$$

while as analyzed also in [49,50] it holds that

$$A_Y^P\equiv D_{\Phi_Z^P\Phi_Z^P} \qquad A_Y^S\equiv D_{\Phi_Z^S\Phi_Z^S} \tag{11a,b}$$

$$A_Z^P\equiv D_{\Phi_Y^P\Phi_Y^P} \qquad A_Z^S\equiv D_{\Phi_Y^S\Phi_Y^S} \tag{11c,d}$$

$$I_x^S\equiv D_{\Phi_x^S\Phi_x^S} \qquad I_x^T\equiv D_{\Phi_x^T\Phi_x^T} \tag{11e,f}$$

Using the expressions of the strain components, the definitions of the stress resultants (eqns. (7)) and applying the principle of virtual work (eqn. (5)), the differential equations of motion in terms of the kinematical components can be written as

$$-E^*Au_{,xx}+\rho\mathrm{A}u_{,tt}=p_x \tag{12a}$$

$$\begin{aligned}&-G\left(A_Y^P+A_Y^S\right)\left(v_{,xx}-\theta_{Z,x}\right)+GA_Y^S\eta_{Y,x}+G\left(D_{\Phi_{CY}^S\Phi_S^S}-D_{\Phi_{CY}^S\Phi_S^T}\right)\left(\eta_{x,x}-\theta_{x,xx}\right)+\\&\quad+GD_{\Phi_{CY}^S\Phi_S^T}\xi_{x,x}+\rho A\left(v_{,tt}-z_C\theta_{x,tt}\right)=p_y\end{aligned} \tag{12b}$$

$$\begin{aligned}&-G\left(A_Z^P+A_Z^S\right)\left(w_{,xx}+\theta_{Y,x}\right)+GA_Z^S\eta_{Z,x}+G\left(D_{\Phi_{CZ}^S\Phi_S^S}-D_{\Phi_{CZ}^S\Phi_S^T}\right)\left(\eta_{x,x}-\theta_{x,xx}\right)+\\&\quad+GD_{\Phi_{CZ}^S\Phi_S^T}\xi_{x,x}+\rho A\left(w_{,tt}+y_C\theta_{x,tt}\right)=p_z\end{aligned} \tag{12c}$$

$$\begin{aligned}&-E^*I_{ZZ}\theta_{Z,xx}-G\left(A_Y^P+A_Y^S\right)\left(v_{,x}-\theta_Z\right)+GA_Y^S\eta_Y+G\left(D_{\Phi_{CY}^S\Phi_S^S}-D_{\Phi_{CY}^S\Phi_S^T}\right)\left(\eta_x-\theta_{x,x}\right)+\\&\quad+GD_{\Phi_{CY}^S\Phi_S^T}\xi_x+\rho I_{ZZ}\theta_{Z,tt}=m_Z\end{aligned} \tag{12d}$$

$$\begin{aligned}&-E^*I_{YY}\theta_{Y,xx}+G\left(A_Z^P+A_Z^S\right)\left(w_{,x}+\theta_Y\right)-GA_Z^S\eta_Z-G\left(D_{\Phi_{CZ}^S\Phi_S^S}-D_{\Phi_{CZ}^S\Phi_S^T}\right)\left(\eta_x-\theta_{x,x}\right)-\\&\quad-GD_{\Phi_{CZ}^S\Phi_S^T}\xi_x+\rho I_{YY}\theta_{Y,tt}=m_Y\end{aligned} \tag{12e}$$

$$\begin{aligned}&-E^*\left(I_{\varphi_{CY}^P\varphi_S^P}\eta_{x,xx}+I_{\varphi_{CY}^P\varphi_{CY}^P}\eta_{Y,xx}+I_{\varphi_{CY}^P\varphi_S^S}\xi_{x,xx}\right)+GA_Y^S\left(\eta_Y-v_{,x}+\theta_Z\right)+\\&\quad+G\left(D_{\Phi_{CY}^S\Phi_S^S}-D_{\Phi_{CY}^S\Phi_S^T}\right)\left(\eta_x-\theta_{x,x}\right)+GD_{\Phi_{CY}^S\Phi_S^T}\xi_x+\end{aligned}$$

$$+\rho\left(I_{\varphi_{CY}^P\varphi_S^P}\eta_{x,tt}+I_{\varphi_{CY}^P\varphi_S^S}\xi_{x,tt}+I_{\varphi_{CY}^P\varphi_{CY}^P}\eta_{Y,tt}\right)=m_{\varphi_{CY}^P} \tag{12f}$$

$$\begin{aligned}&-E^*\left(I_{\varphi_{CZ}^P\varphi_S^P}\eta_{x,xx}+I_{\varphi_{CZ}^P\varphi_{CZ}^P}\eta_{Z,xx}+I_{\varphi_{CZ}^P\varphi_S^S}\xi_{x,xx}\right)+GA_Z^S\left(\eta_Z-w_{,x}-\theta_Y\right)+\\&+G\left(D_{\Phi_{CZ}^S\Phi_S^S}-D_{\Phi_{CZ}^S\Phi_S^T}\right)\left(\eta_x-\theta_{x,x}\right)+GD_{\Phi_{CZ}^S\Phi_S^T}\xi_x+\\&+\rho\left(I_{\varphi_{CZ}^P\varphi_S^P}\eta_{x,tt}+I_{\varphi_{CZ}^P\varphi_S^S}\xi_{x,tt}+I_{\varphi_{CZ}^P\varphi_{CZ}^P}\eta_{Z,tt}\right)=m_{\varphi_{CZ}^P}\end{aligned} \tag{12g}$$

$$\begin{aligned}&-G\left(I_t^P+I_t^S+I_t^T\right)\theta_{x,xx}+G\left(I_t^S+I_t^T\right)\left(\eta_x-\theta_{x,x}\right)-GI_t^T\xi_{x,x}+\\&+G\left(D_{\Phi_{CY}^S\Phi_S^S}-D_{\Phi_{CY}^S\Phi_S^T}\right)\left(\eta_{Y,x}-v_{,xx}+\theta_{Z,x}\right)+G\left(D_{\Phi_{CZ}^S\Phi_S^S}-D_{\Phi_{CZ}^S\Phi_S^T}\right)\cdot\\&\cdot\left(\eta_{Z,x}-w_{,xx}-\theta_{Y,x}\right)+\rho\left[A\left(-z_C v_{,tt}+y_C w_{,tt}\right)+I_p\theta_{x,tt}\right]=m_t\end{aligned} \tag{12h}$$

$$\begin{aligned}&-E^*\left(I_{\varphi_S^P\varphi_S^P}\eta_{x,xx}+I_{\varphi_{CY}^P\varphi_S^P}\eta_{Y,xx}+I_{\varphi_{CZ}^P\varphi_S^P}\eta_{Z,xx}\right)+G\left(I_t^S+I_t^T\right)\left(\eta_x-\theta_{x,x}\right)-GI_t^T\xi_x+\\&+G\left(D_{\Phi_{CY}^S\Phi_S^S}-D_{\Phi_{CY}^S\Phi_S^T}\right)\left(\eta_Y-v_{,x}+\theta_Z\right)+G\left(D_{\Phi_{CZ}^S\Phi_S^S}-D_{\Phi_{CZ}^S\Phi_S^T}\right)\cdot\\&\cdot\left(\eta_Z-w_{,x}-\theta_Y\right)+\rho\left(I_{\varphi_S^P\varphi_S^P}\eta_{x,tt}+I_{\varphi_{CY}^P\varphi_S^P}\eta_{Y,tt}+I_{\varphi_{CZ}^P\varphi_S^P}\eta_{Z,tt}\right)=m_{\varphi_S^P}\end{aligned} \tag{12i}$$

$$\begin{aligned}&-E^*\left(I_{\varphi_{CY}^P\varphi_S^S}\eta_{Y,xx}+I_{\varphi_{CZ}^P\varphi_S^S}\eta_{Z,xx}+I_{\varphi_S^S\varphi_S^S}\xi_{x,xx}\right)+GI_t^T\left(\xi_x-\eta_x+\theta_{x,x}\right)+\\&+GD_{\Phi_{CY}^S\Phi_S^T}\left(\eta_Y-v_{,x}+\theta_Z\right)+GD_{\Phi_{CZ}^S\Phi_S^T}\left(\eta_Z-w_{,x}-\theta_Y\right)+\\&+\rho\left(I_{\varphi_S^S\varphi_S^S}\xi_{x,tt}+I^{\rho}_{\varphi_{CY}^P\varphi_S^S}\eta_{Y,tt}+I^{\rho}_{\varphi_{CZ}^P\varphi_S^S}\eta_{Z,tt}\right)=m_{\varphi_S^S}\end{aligned} \tag{12j}$$

where the externally applied dynamic loads are related to the components of the traction vector applied on the lateral surface of the beam t_x, t_y, t_z as

$$p_i\left(x,t\right)=\int_\Gamma t_i\,\mathrm{d}s,\quad i=x,y,z \tag{13a}$$

$$m_t\left(x,t\right)=\int_\Gamma t_z y-t_y z\,\mathrm{d}s \tag{13b}$$

$$m_Y\left(x,t\right)=\int_\Gamma t_x Z\,\mathrm{d}s \qquad m_Z\left(x,t\right)=-\int_\Gamma t_x Y\,\mathrm{d}s \tag{13c,d}$$

$$m_i\left(x,t\right)=\int_\Gamma t_x\left(i\right)\mathrm{d}s,\quad i=\varphi_S^P,\varphi_S^S,\varphi_{CY}^P,\varphi_{CZ}^P \tag{13e}$$

The above governing differential equations (eqns. (12)) are also subjected to the initial conditions ($x\in\left(0,l\right)$)

$$u\left(x,0\right)=u_0\left(x\right) \qquad u_{,t}\left(x,0\right)=u_{0,t}\left(x\right) \tag{14a,b}$$

$$v\left(x,0\right)=v_0\left(x\right) \qquad v_{,t}\left(x,0\right)=v_{0,t}\left(x\right) \tag{14c,d}$$

$$\theta_Z\left(x,0\right)=\theta_{Z0}\left(x\right) \qquad \theta_{Z,t}\left(x,0\right)=\theta_{Z0,t}\left(x\right) \tag{14e,f}$$

$$w\left(x,0\right)=w_0\left(x\right) \qquad w_{,t}\left(x,0\right)=w_{0,t}\left(x\right) \tag{14g,h}$$

$$\theta_Y(x,0)=\theta_{Y0}(x) \qquad \theta_{Y,t}(x,0)=\theta_{Y0,t}(x) \qquad (14i,j)$$

$$\theta_x(x,0)=\theta_{x0}(x) \qquad \theta_{x,t}(x,0)=\theta_{x0,t}(x) \qquad (14k,l)$$

$$\eta_x(x,0)=\eta_{x0}(x) \qquad \eta_{x,t}(x,0)=\eta_{x0,t}(x) \qquad (14m,n)$$

$$\xi_x(x,0)=\xi_{x0}(x) \qquad \xi_{x,t}(x,0)=\xi_{x0,t}(x) \qquad (14o,p)$$

together with the corresponding boundary conditions of the problem at hand, which are given as

$$a_1 u+\alpha_2 N_b=\alpha_3 \qquad (15a)$$

$$\beta_1 v+\beta_2 V_{by}=\beta_3 \qquad \gamma_1 w+\gamma_2 V_{bz}=\gamma_3 \qquad (15b,c)$$

$$\overline{\beta}_1\theta_Z+\overline{\beta}_2 M_{bZ}=\overline{\beta}_3 \qquad \overline{\gamma}_1\theta_Y+\overline{\gamma}_2 M_{bY}=\overline{\gamma}_3 \qquad (15d,e)$$

$$\tilde{\beta}_1\eta_Z+\tilde{\beta}_2 M_{b\varphi_{CZ}^P}=\tilde{\beta}_3 \qquad \tilde{\gamma}_1\eta_Y+\tilde{\gamma}_2 M_{b\varphi_{CY}^P}=\tilde{\gamma}_3 \qquad (15f,g)$$

$$\delta_1\theta_x+\delta_2 M_{bt}=\delta_3 \qquad \overline{\delta}_1\eta_x+\overline{\delta}_2 M_{b\varphi_S^P}=\overline{\delta}_3 \qquad \tilde{\delta}_1\xi_x+\tilde{\delta}_2 M_{b\varphi_S^S}=\tilde{\delta}_3 \qquad (15h,i,j)$$

at the beam ends $x=0,l$, where N_b, V_{by}, V_{bz}, M_{bZ}, M_{bY}, $M_{b\varphi_{CY}^P}$, $M_{b\varphi_{CZ}^P}$, M_{bt}, $M_{b\varphi_S^P}$, $M_{b\varphi_S^S}$ are the reaction forces, moments and warping moments respectively.

Finally, α_k, β_k, $\overline{\beta}_k, \tilde{\beta}_k$ γ_k, $\overline{\gamma}_k$, $\tilde{\gamma}_k, \delta_k, \overline{\delta}_k, \tilde{\delta}_k$ $(k=1,2,3)$ are functions specified at the boundaries of the beam ($x=0,l$). The boundary conditions (15) are the most general boundary conditions for the problem at hand, including also the elastic support. It is apparent that all types of the conventional boundary conditions (clamped, simply supported, free or guided edge) can be derived from these equations by specifying appropriately these functions (e.g. for a clamped edge it is $\alpha_1=\beta_1=\overline{\beta}_1=\tilde{\beta}_1=\gamma_1=\overline{\gamma}_1=\tilde{\gamma}_1=\delta_1=\overline{\delta}_1=\tilde{\delta}_1=1$, $\alpha_2=\alpha_3=\beta_2=\beta_3=\overline{\beta}_2=\overline{\beta}_3=\tilde{\beta}_2=$
$=\tilde{\beta}_3=\gamma_2=\overline{\gamma}_3=\tilde{\gamma}_2=\tilde{\gamma}_3=\delta_2=\delta_3=\overline{\delta}_2=\overline{\delta}_3=\tilde{\delta}_2=\tilde{\delta}_3=0$).

2.3 Warping functions due to shear Φ_{CY}^P, Φ_{CZ}^P, Φ_{CY}^S, Φ_{CZ}^S

The analysis described in the previous section presumes that the warping functions Φ_{CY}^P, Φ_{CZ}^P, Φ_{CY}^S, Φ_{CZ}^S with respect to the centroidal principal bending system $CXYZ$ are already established. According to the procedure presented in [49, 50], examining each primary warping function Φ_{Ci}^P $(i=Y,Z)$ separately, a boundary value problem in each direction is formulated as

$$\nabla^2\overline{\Phi}_{CY}^P=Z \qquad \overline{\Phi}_{CY,n}^P=0 \qquad \text{on the boundary} \qquad (17a,b)$$

$$\nabla^2\overline{\Phi}_{CZ}^P=Y \qquad \overline{\Phi}_{Z,n}^P=0 \qquad \text{on the boundary} \qquad (18a,b)$$

where $\overline{\Phi}_{CY}^P=-\left(I_{YY}/A_Z^P\right)\Phi_{CY}^P$, $\overline{\Phi}_{CZ}^P=-\left(I_{ZZ}/A_Y^P\right)\Phi_{CZ}^P$, while $(\cdot)_{,n}$ indicates the derivative with respect to the outward normal vector to the boundary **n** (directional derivative). After establishing $\overline{\Phi}_{Ci}^P$ $(i=Y,Z)$, geometric constants A_i^P $(i=Y,Z)$ can be evaluated employing definition (8i) as

$$A_Y^P = \frac{\left(I_{ZZ}\right)^2}{D_{\bar{\Phi}_Z^P \bar{\Phi}_Z^P}} \qquad A_Z^P = \frac{\left(I_{YY}\right)^2}{D_{\bar{\Phi}_Y^P \bar{\Phi}_Y^P}} \tag{19a,b}$$

Moreover, after evaluating Φ_{Ci}^P $(i = Y, Z)$, warping functions φ_{Ci}^P $(i = Y, Z)$ can be established through eqns. (4c,d).

Subsequently, φ_{Ci}^S $(i = Y, Z)$ employed in order to correct shear stresses are indirectly computed through Φ_{Ci}^S $(i = Y, Z)$ which can be established by formulating the following boundary value problem in each direction

$$\nabla^2 \tilde{\Phi}_{Ci}^S = \varphi_{Ci}^P, \ (i = Y, Z) \qquad \tilde{\Phi}_{Ci,n}^S = 0 \qquad \text{on the boundary} \tag{20a,b}$$

while it holds that $\bar{\Phi}_{CY}^S = \tilde{\Phi}_{CY}^S + Z\left(I_{\varphi_{CY}^P \varphi_{CY}^P} \Big/ A_Z^P\right)$, $\bar{\Phi}_{CZ}^S = \tilde{\Phi}_{CZ}^S + Y\left(I_{\varphi_{CZ}^P \varphi_{CZ}^P} \Big/ A_Y^P\right)$ and $\bar{\Phi}_{CY}^S = -\left(I_{\varphi_{CY}^P \varphi_{CY}^P} \Big/ A_Z^S\right)\Phi_{CY}^S$, $\bar{\Phi}_{CZ}^S = -\left(I_{\varphi_{CZ}^P \varphi_{CZ}^P} \Big/ A_Y^S\right)\Phi_{CZ}^S$. After establishing $\bar{\Phi}_{Ci}^S$, the geometric constants A_i^S $(i = Y, Z)$ can be evaluated employing definition (8i) as

$$A_Y^S = \frac{\left(I_{\varphi_{CZ}^P \varphi_{CZ}^P}\right)^2}{D_{\bar{\Phi}_{CZ}^S \bar{\Phi}_{CZ}^S}} \qquad A_Z^S = \frac{\left(I_{\varphi_{CY}^P \varphi_{CY}^P}\right)^2}{D_{\bar{\Phi}_{CY}^S \bar{\Phi}_{CY}^S}} \tag{21}$$

2.4 Warping functions due to torsion φ_S^P, Φ_S^S, Φ_S^T

Similarly with the previous section, the torsional warping functions are established independently as follows. φ_S^P is given by the following boundary value problem (St. Venant problem of uniform torsion) as

$$\nabla^2 \varphi_S^P = 0 \qquad \varphi_{S,n}^P = z n_y - y n_z \qquad \text{on the boundary} \tag{22a,b}$$

It is noticed that in order for φ_S^P to be the primary torsional warping function, the analysis has to be carried out with respect to the center of twist S, which is initially specified according to the procedure presented in [11]. Following the strategy presented in the previous section, Φ_S^S can be established by formulating the following boundary value problem as

$$\nabla^2 \bar{\Phi}_S^S = \varphi_S^P \qquad \bar{\Phi}_{S,n}^S = 0 \qquad \text{on the boundary} \tag{23a,b}$$

where $\bar{\Phi}_S^S = -\left(I_{\varphi_S^P \varphi_S^P} \Big/ I_t^S\right)\Phi_S^S$. Employing eqn. (8i), I_t^S is evaluated as

$$I_t^S = \frac{\left(I_{\varphi_S^P \varphi_S^P}\right)^2}{D_{\bar{\Phi}_S^S \bar{\Phi}_S^S}} \tag{24}$$

while, after evaluating Φ_S^S, φ_S^S can be established through eqn. (4a). The final boundary value problem for Φ_S^T is constructed as

$$\nabla^2\tilde{\Phi}_S^T = \varphi_S^S \qquad \tilde{\Phi}_{S,n}^T = 0 \qquad \text{on the boundary} \tag{25a,b}$$

while it holds that $\bar{\Phi}_S^T = \tilde{\Phi}_S^T + \varphi_S^P \left(I_{\varphi_S^S \varphi_S^S} \Big/ I_t^S \right)$ and $\bar{\Phi}_S^T = -\left(I_{\varphi_S^S \varphi_S^S} \Big/ I_t^T \right) \Phi_S^T$. Finally, employing definition (10b), I_t^T is evaluated as

$$I_t^T = \frac{\left(I_{\varphi_S^S \varphi_S^S} \right)^2}{D_{\bar{\Phi}_S^T \bar{\Phi}_S^T}} \tag{26}$$

It is remarked that all boundary value problems (17), (18), (20), (22), (23), (25) have solution, since the condition $\int_\Gamma \left(i_{,n} \right) \mathrm{d}s = 0$, ($i = \bar{\Phi}_j^P, \tilde{\Phi}_j^S, \varphi_x^P, \bar{\Phi}_x^S, \tilde{\Phi}_x^T$, $j = Y, Z$, $m, n = 1, ..., M$) [21] is satisfied. It is also worth here noting that, since the problems (17), (18), (20), (22), (23), (25) have Neumann type boundary conditions, each warping function contains an arbitrary integration constant indicating a parallel displacement of the cross section along the beam axis. The evaluation of these constants is performed as presented in [11].

3 NUMERICAL SOLUTION

According to the precedent analysis, the flexural-torsional dynamic analysis of beams of arbitrary composite cross section including generalized warping effects reduces in establishing the components $u(x,t)$, $v(x,t)$, $w(x,t)$, $\theta_X(x,t)$, $\theta_Z(x,t)$, $\theta_Y(x,t)$, $\eta_x(x,t)$, $\eta_Y(x,t)$, $\eta_Z(x,t)$ and $\xi_x(x,t)$ having continuous derivatives up to the second order with respect to x at the interval $(0,l)$ and up to the first order at $x = 0, l$ and up to the second order with respect to t, satisfying the initial-boundary value problem described by the coupled governing differential equations of equilibrium (eqns. (12)) along the beam, the initial conditions (eqns. (14)) and the boundary conditions (eqns. (15)) at the beam ends $x = 0, l$. Eqns. (12), (14), (15) are solved using the Analog Equation Method [52]. Application of the boundary element technique yields a system of linear coupled differential-algebraic equations of motion which can be solved employing any efficient time-integration scheme (e.g. Mean Acceleration Method). The geometric constants defined in eqns. (8) are evaluated by converting the domain integrals into line ones along the boundary using integration by parts, the Gauss theorem and the Green identity. The expressions of these constants are given in the appendix A of [50].

4 NUMERICAL EXAMPLES

On the basis of the analytical and numerical procedures presented in the previous sections, a computer program has been written and representative examples have been studied. A commercial FEM package with solid and beam modeling capabilities [51] is employed to compare and verify the results of the proposed method.

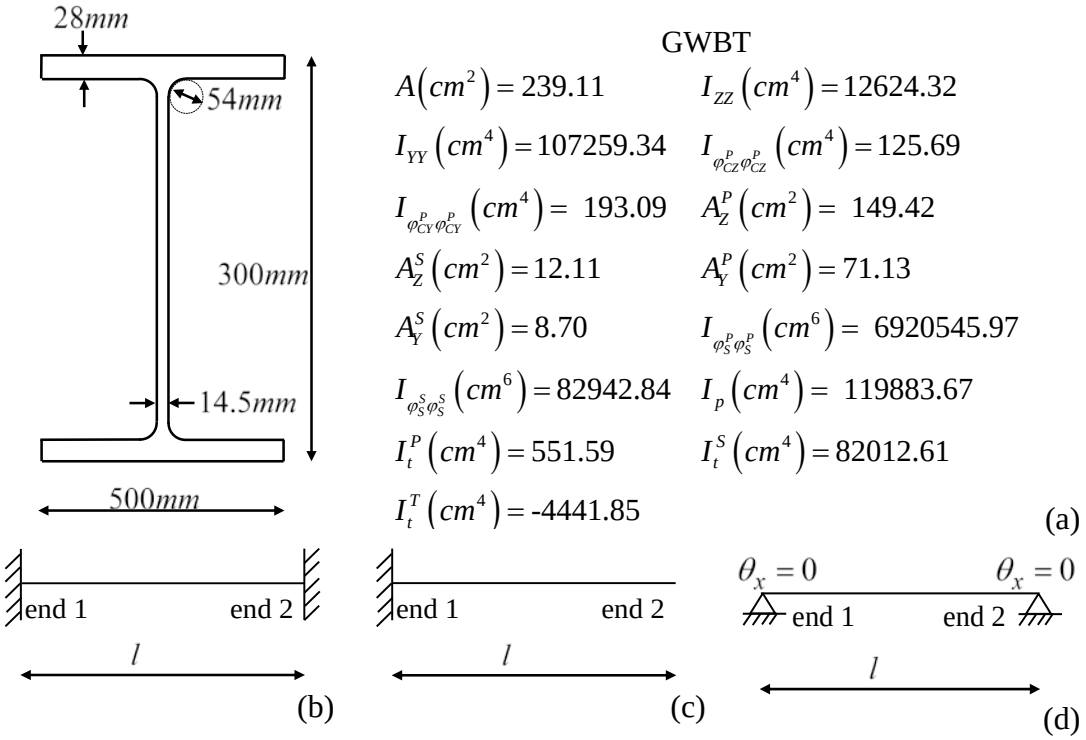

Fig. 3. Cross sections of beams of examples 1 (a) along with three types of boundary conditions (b-d).

Example 1

In the first example, the free vibration characteristics of four HEB500 cross section (Fig. 3a) steel ($E = 210GPa$, $G = 80.8GPa$, $\nu = 0.3$, $\rho = 7.85kN\,sec^2/m^4$) beams of lengths $l = 2.5m, 3.5m, 4.5m, 5.5m$ for three types of boundary conditions (clamped at both ends (Fig. 3b), cantilever (Fig. 3c), simply supported with fixed torsional rotation (Fig. 3d)) have been analyzed. More specifically, the generalized eigenvalue problem of eqn(35) has been solved to obtain the natural frequencies for the Generalized Warping Beam Theory (GWBT). For comparison reasons Timoshenko Beam Theory (TBT [51]) and Solid (3-D hexahedral elements extruded by quadrilateral surfaces) FEM (Solid FEM [51]) models have been analyzed. In the Solid models, rigid diaphragms at every set of nodes having the same longitudinal coordinate have been employed, pointing out that the diaphragms are designed so as each set of nodes has the same translation and rotation in the cross section plane, corresponding to the assumption employed in the proposed method that the cross section maintains its shape at the transverse directions during deformation (no distortion). In GWBT solutions 88 elements have been used while in TBT [51] 100 elements per meter of length. The number of Solid FEM [51] elements that have been used is 24300. There are three types of natural frequencies under examination, namely bending natural frequencies with deflections along the y (v natural frequencies) and the z axis (w natural frequencies) and torsional natural frequencies (θ_x natural frequencies).

Table 1. Discrepancies (%) of natural frequencies between GWBT- Solid FEM [51] and TBT [51]- Solid FEM [51] of the clamped beam of example 1 for various lengths.

Natural frequency type	l=2.5m		l=3.5m		l=4.5m		l=5.5m	
	GWBT	TBT	GWBT	TBT	GWBT	TBT	GWBT	TBT
1st v	-0.04	11.46	-0.21	12.48	-0.39	12.96	-0.59	13.23
2nd v	0.07	9.25	-0.14	11.00	-0.34	11.96	-0.56	12.52
3rd v	0.16	7.43	-0.08	9.50	-0.29	10.83	-0.52	11.67
4th v	0.23	6.02	-0.02	8.12	-0.25	9.68	-0.48	10.75
1st w	0.77	4.35	0.44	5.61	0.26	6.99	0.17	8.21
2nd w	1.10	3.36	0.71	3.80	0.48	4.63	0.33	5.59
3rd w	1.16	3.38	0.77	3.36	0.56	3.78	0.41	4.39
4th w	1.24	3.19	0.80	14.34	0.58	3.17	0.44	3.59
1st θ_x	-0.64	54.61	-1.35	54.29	-0.22	52.42	-0.39	49.93
2nd θ_x	0.17	30.71	-0.11	36.00	-0.30	37.73	-0.46	38.03
3rd θ_x	-1.14	12.06	-1.99	22.40	0.14	26.93	-0.38	29.09
4th θ_x	0.49	-5.02	0.10	-39.43	-0.19	17.69	-0.43	21.57

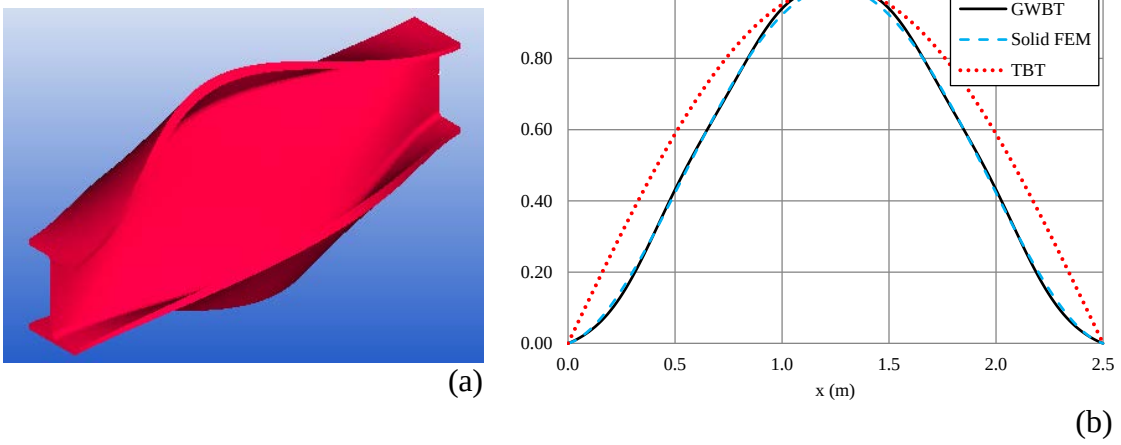

Fig. 4. 1st torsional modeshape of the clamped beam of length $l = 2.5m$ of example 1 as obtained from Solid FEM [51] (a) in comparison with those obtained by GWBT and TBT [51] (b).

In Tables 1, 2 and 3the natural frequencies as obtained from GWBT and TBT [51] are compared with Solid FEM [51] solutions for the clamped, cantilever and simply supported boundary condition, respectively. Figs. 4a and 4b illustrate the 1st torsional modeshape of bar of length $l = 2.5m$ of example 1 as obtained from Solid FEM [51] and comparison among those obtained by GWBT and TBT [51] and Solid FEM [51] , respectively. Figs. 5a, 5b and 6c illustrate the first four bending natural frequencies with deflections along the y axis, the z axis and torsional natural frequencies, respectively as obtained from GWBT, TBT [51] and Solid FEM [51] solutions for the clamped boundary condition. Figs. 6a and 6b show the first four torsional natural frequencies for the cantilever boundary condition and the first four bending natural frequencies with deflections along the y axis for the simply supported

boundary condition, respectively, as calculated by GWBT, TBT [51] and Solid FEM [51] solutions.

From the results of Tables 1-3, it is concluded that TBT [51] can not predict the natural frequencies as accurate as GWBT can. In more detail the discrepancies of GWBT with respect to Solid solutions is up to 2.00% (absolute value) for any of the examined boundary condition or length. On the contrast the discrepancies of TBT [51] with respect to Solid FEM [51] solutions is up to 54.61% for Table 1, 52.49% for Table 2 and 16.91% for Table 3 (absolute values).

Table 2. Discrepancies (%) of natural frequencies between GWBT- Solid FEM [51] and TBT [51]- Solid of the cantilever beam of example 1 for various lengths.

Natural frequency type	l=2.5m		l=3.5m		l=4.5m		l=5.5m	
	GWBT	TBT	GWBT	TBT	GWBT	TBT	GWBT	TBT
1^{st} v	-0.15	13.39	-0.27	13.58	-0.42	13.66	-0.61	13.70
2^{nd} v	-0.09	11.39	-0.24	12.48	-0.41	12.97	-0.60	13.24
3^{rd} v	-0.02	9.16	-0.20	11.03	-0.38	12.01	-0.58	12.57
4^{th} v	0.05	7.05	-0.15	9.41	-0.34	10.83	-0.56	11.70
1^{st} w	0.13	9.88	0.07	11.46	0.04	12.30	0.02	12.77
2^{nd} w	0.54	2.90	0.29	5.17	0.17	7.04	0.09	8.49
3^{rd} w	0.56	2.09	0.36	3.35	0.24	4.62	0.16	5.82
4^{th} w	0.54	-0.47	0.37	1.68	0.26	2.88	0.18	3.93
1^{st} θ_x	0.13	52.49	0.20	42.86	0.21	36.37	0.29	31.75
2^{nd} θ_x	-0.06	31.13	-0.17	31.13	-0.25	29.58	-0.40	27.62
3^{rd} θ_x	0.00	16.11	-0.16	21.44	-0.27	23.22	-0.35	23.58
4^{th} θ_x	0.21	1.42	-0.12	11.73	-0.33	16.24	-0.55	18.39

Table 3. Discrepancies (%) of natural frequencies between GWBT- Solid FEM [51] and TBT [51]- Solid FEM [51] of the simply supported beam of example 1 for various lengths.

Natural frequency type	l=2.5m		l=3.5m		l=4.5m		l=5.5m	
	GWBT	TBT	GWBT	TBT	GWBT	TBT	GWBT	TBT
1^{st} v	-0.14	12.98	-0.27	13.36	-0.43	13.53	-0.62	13.62
2^{nd} v	-0.10	11.04	-0.24	12.25	-0.41	12.83	-0.61	13.14
3^{rd} v	-0.06	8.84	-0.21	10.76	-0.38	11.82	-0.59	12.43
4^{th} v	-0.02	6.94	-0.18	9.21	-0.36	10.65	-0.57	11.56
1^{st} w	-0.01	7.34	0.00	9.53	0.01	10.88	0.00	11.71
2^{nd} w	-0.05	3.19	-0.04	4.97	-0.04	6.63	-0.03	8.01
3^{rd} w	-0.05	2.01	-0.07	2.93	-0.07	4.11	-0.07	5.30
4^{th} w	0.00	1.83	-0.07	2.13	-0.08	2.84	-0.09	3.70
1^{st} θ_x	-0.10	9.81	-0.08	9.64	-0.06	8.79	-0.04	7.79
2^{nd} θ_x	-0.16	4.63	-0.24	8.35	-0.33	9.61	-0.42	9.93
3^{rd} θ_x	-0.15	-4.64	-0.25	3.54	-0.38	7.04	-0.52	8.72
4^{th} θ_x	-0.15	-16.19	-0.24	-3.07	-0.38	2.94	-0.53	6.10

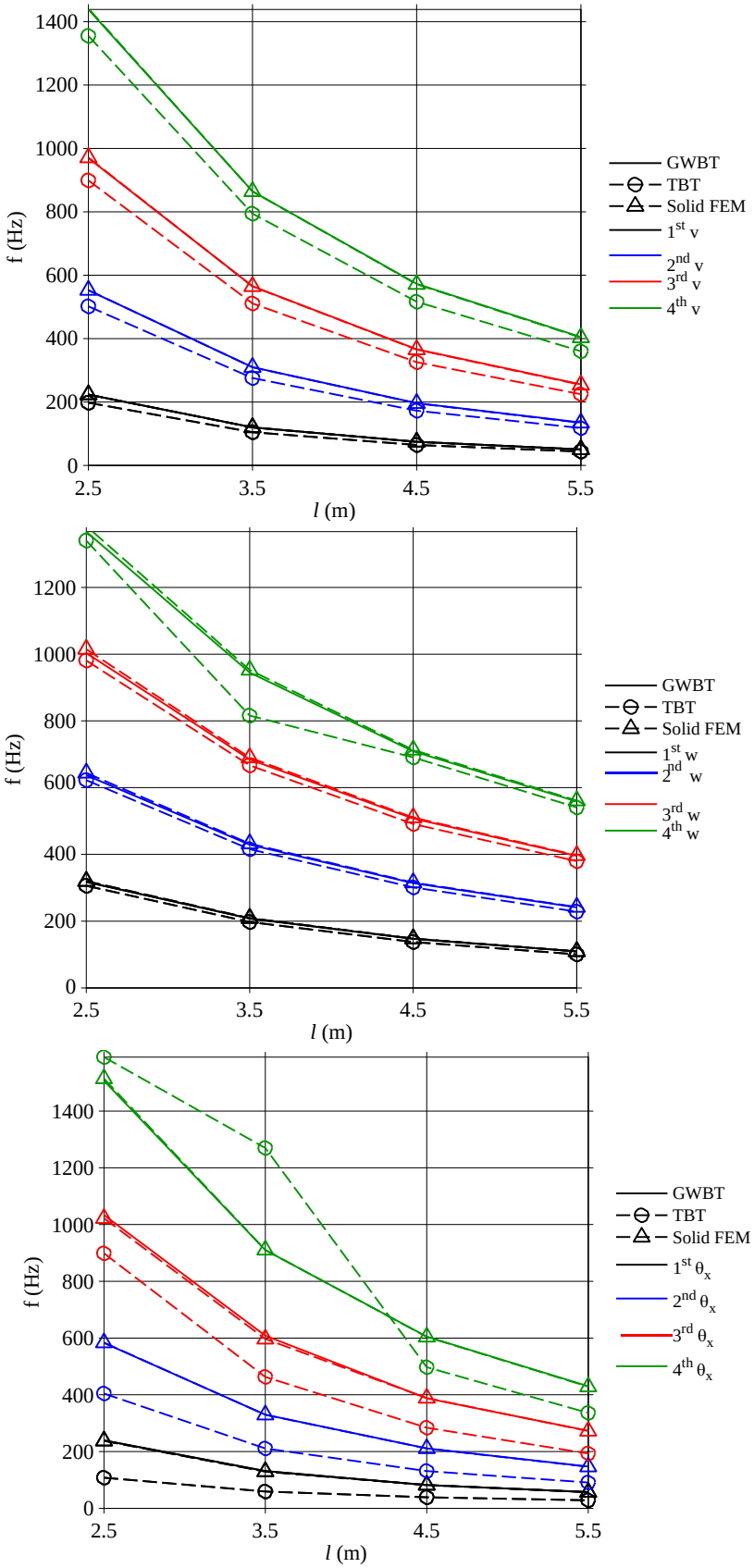

Fig. 5. Comparison of first four bending natural frequencies with deflections along the y axis (a) and the z axis (b) and first four torsional natural frequencies among GWBT, TBT [51] and Solid FEM [51] solutions of clamped beam of example 1 for various lengths.

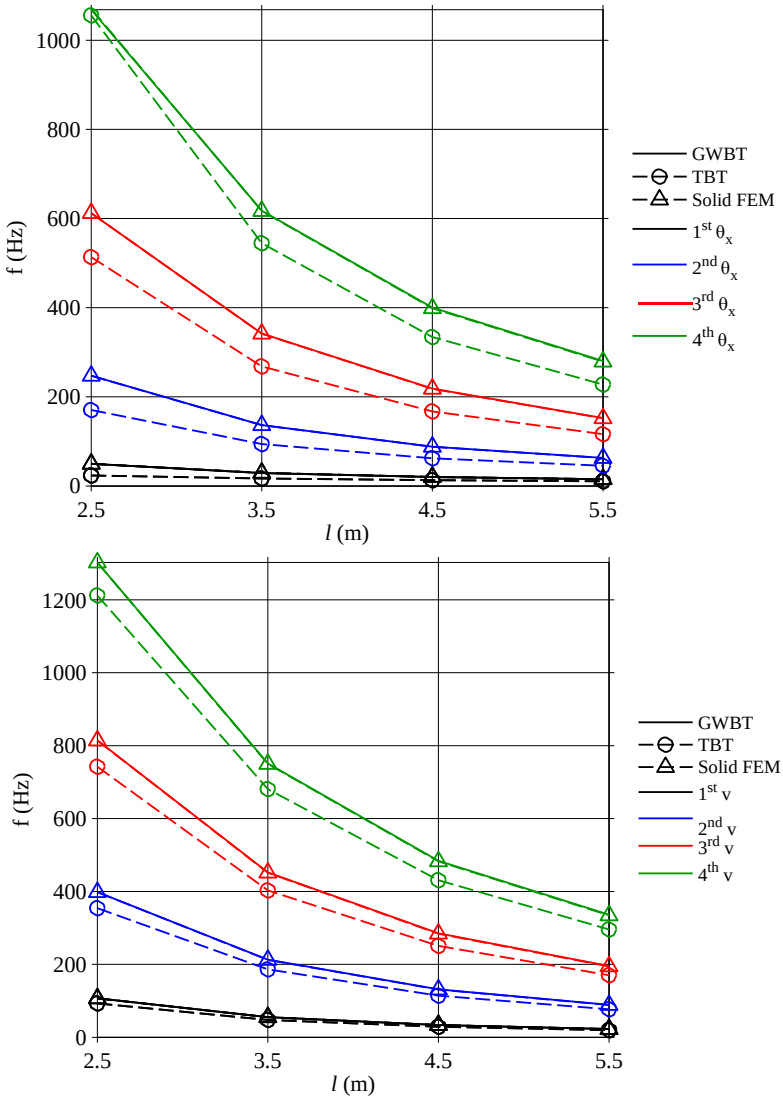

Fig. 6. Comparison of first four torsional natural frequencies of cantilever beam of example 1 (a) and of first four bending natural frequencies with deflections along the y axis of simply supported beam of example 1 for various lengths among GWBT, TBT [51] and Solid FEM [51] solutions.

Example 2

As a final example, the forced vibrations of a box shaped cross section (Fig. 7a) steel ($E = 21\,GPa$, $G = 8.08\,GPa$, $v = 0.3$, $\rho = 2.5\,kN\,sec^2/m^4$) beam of length $l = 30m$, clamped at end 1 and simply supported with fixed torsional rotation at end 2 (Fig 7b), have been examined. The beam is subjected to a uniform distributed dynamic load $p_z(t)$ (Fig 7a, b) along the axis of symmetry Z . Three load cases have been examined (Fig 7c). The time history of loading is constant for load case I and sinusoidal for load cases II and III. The frequency of load case III is $51.48\,rad/\sec$ that is very close to the first natural frequency as calculated by model B ($56.44\,rad/\sec$) while it is not valid for load case II that is $30.00\,rad/\sec$.

More specifically, the initial boundary value problem of eqns(12),(14),(15) has been solved to obtain the response of Generalized Warping Beam Theory (GWBT). For comparison reasons Timoshenko Beam Theory (TBT [51]) and Solid (3-D hexahedral elements extruded by quadrilateral surfaces) FEM [51] models have been analyzed. In the Solid model, rigid dia-

phragms at every set of nodes with the same properties as in the first example have been used. In GWBT solution 62 elements have been employed as in TBT [51]. The number of Solid FEM [51] elements that have been used is 16400.

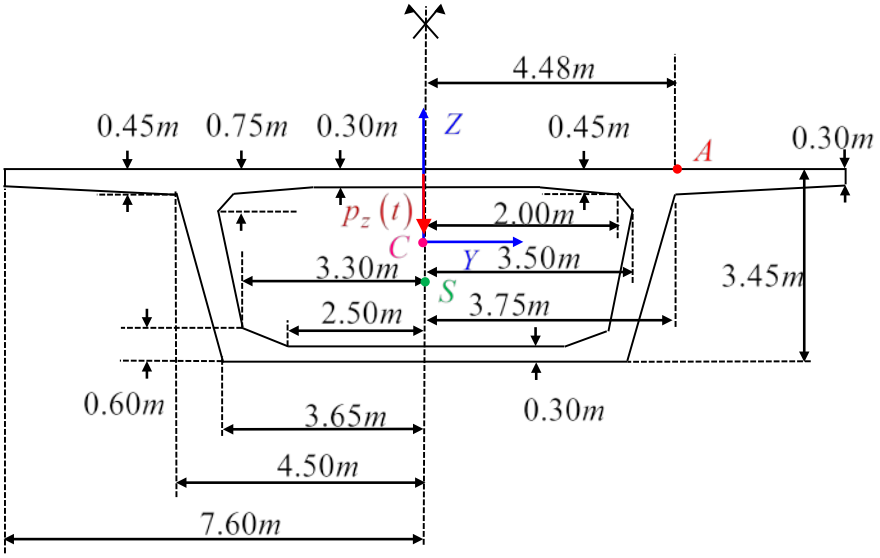

Model B

$A(m^2)=11.28$ $I_{ZZ}(m^4)=169.89$ $I_{YY}(m^4)=19.07$

$I_{\varphi^P_{CZ}\varphi^P_{CZ}}(m^4)=1.20$ $I_{\varphi^P_{CY}\varphi^P_{CY}}(m^4)=3.36$ $A^P_Z(m^2)=2.61$

$A^S_Z(m^2)=29.74$ $A^P_Y(m^2)=6.76$ $A^S_Y(m^2)=0.77$

$I_{\varphi^P_S\varphi^P_S}(m^6)=62.74$ $I_{\varphi^S_S\varphi^S_S}(m^6)=14.22$ $I_p(m^4)=192.83$

$I^P_t(m^4)=42.46$ $I^S_t(m^4)=27.05$ $I^T_t(m^4)=1.21$

(a)

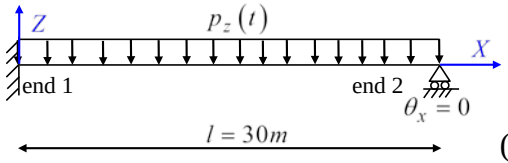

(b)

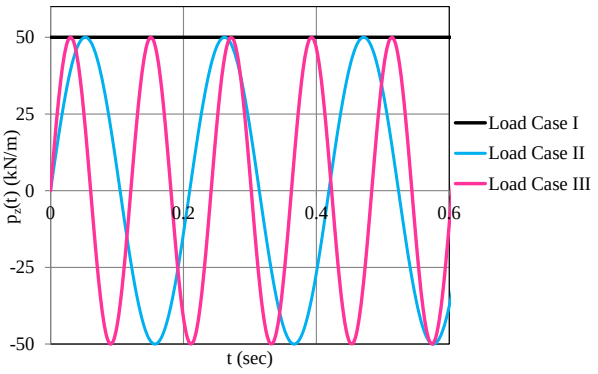

(c)

Fig. 7. Cross section (a), boundary conditions and loading (b), load cases (c) of the beam of example 2.

Figs. 8a, 10a and 11a illustrate the time history of the displacement w at $x=16.94m$ (position of maximum displacement) for Load Cases I, II and III, respectively.

Figs. 8b, 10b and 11b illustrate the time history of normal stress σ_{xx} at the point A (see Fig. 7a) at $x=1.5m$ of the beam for Load Cases I, II and III, respectively. From these figures, it is deduced the results of the Solid FEM [51] solution are closer to the proposed methodology (GWBT) than the TBT [51], so the effect of Generalized Warping is pronounced.

Figs. 9a, 9b and 9c show the distribution of normal stresses σ_{xx} at $x = 1.5m$ for Load Case I acording to Solid FEM, GWBT and Timoshenko solutions, respectively, at time instances that appears the maximum stress at point A for each solution. The discrepancies of the distribution and the extreme values of GWBT and TBT [51] with respect to Solid FEM [51] solutions indicates that GWBT is much more appropriate for the analysis than the TBT [51].

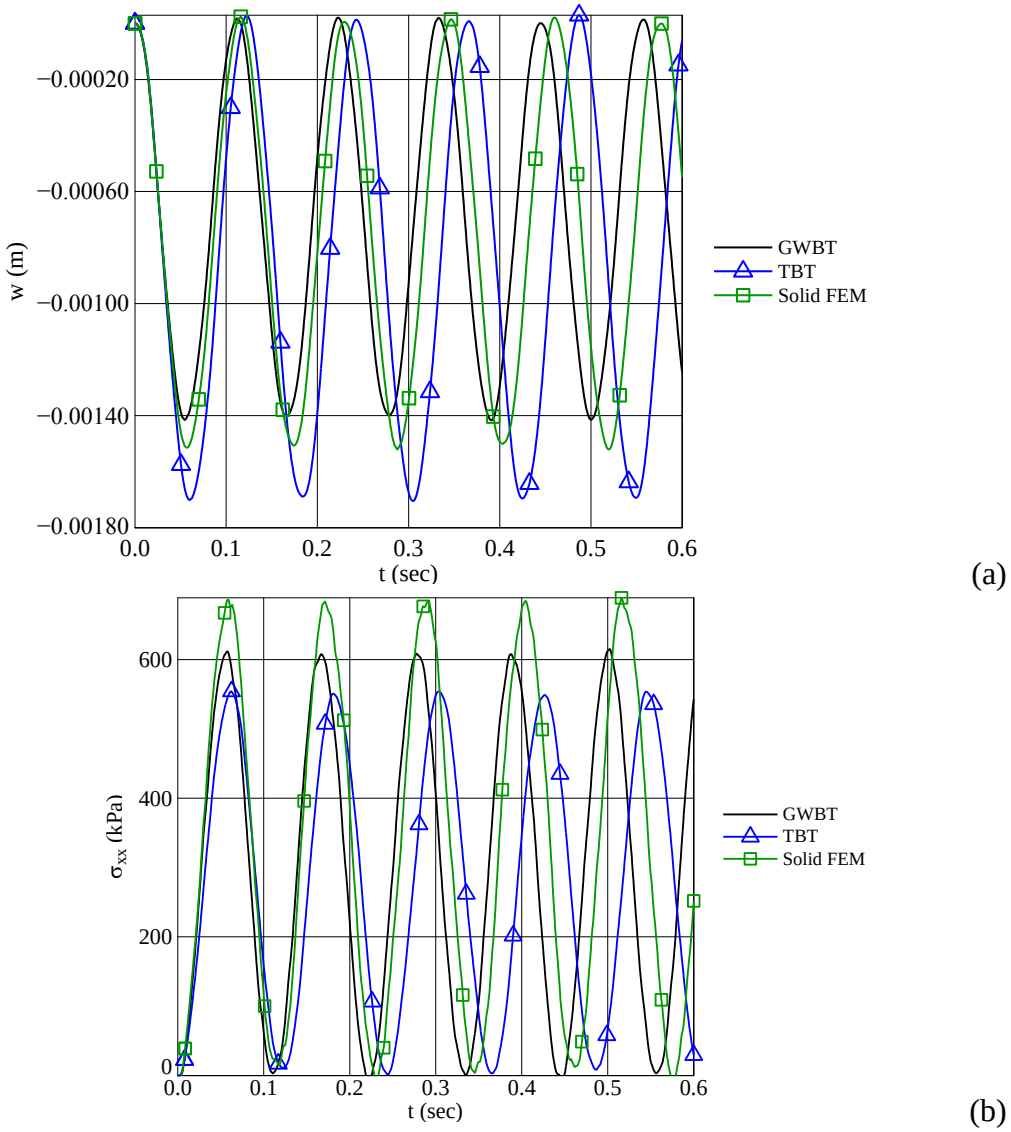

Fig. 8. Time history of the displacement w at $x = 16.94m$ (a) and normal stress σ_{xx} at the point A at $x = 1.5m$ (b) of the beam of example 2 for Load Case I.

5 CONCLUSIONS

In this paper a boundary element solution is developed for the nonuniform warping dynamic analysis of arbitrary cross section beams including shear lag effects due to both flexure and torsion. The beam is subjected to arbitrarily distributed or concentrated external loading, and its ends are supported by the most general boundary conditions. The formulation based on displacements stems from an improved stress field and is capable of yielding more accurate stress component values. The main conclusions that can be drawn from this investigation are

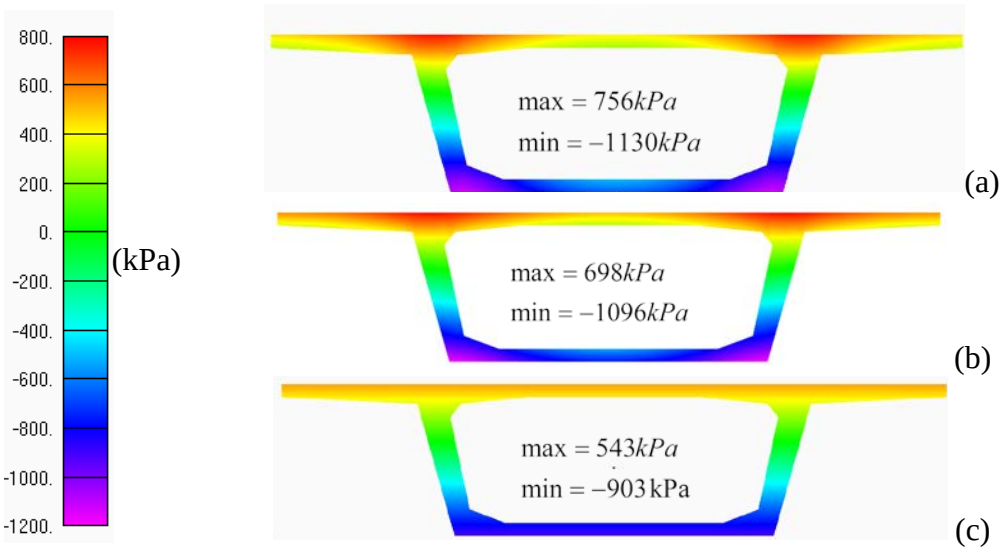

Fig. 9. Distribution of normal stresses σ_{xx} at $x = 1.5m$ for Load Case I of example 2, acording to Solid FEM [51] (a), GWBT (b) and TBT [51] (c) solutions at time instances 0.516sec, 0.5025sec and 0.0624sec, respectively.

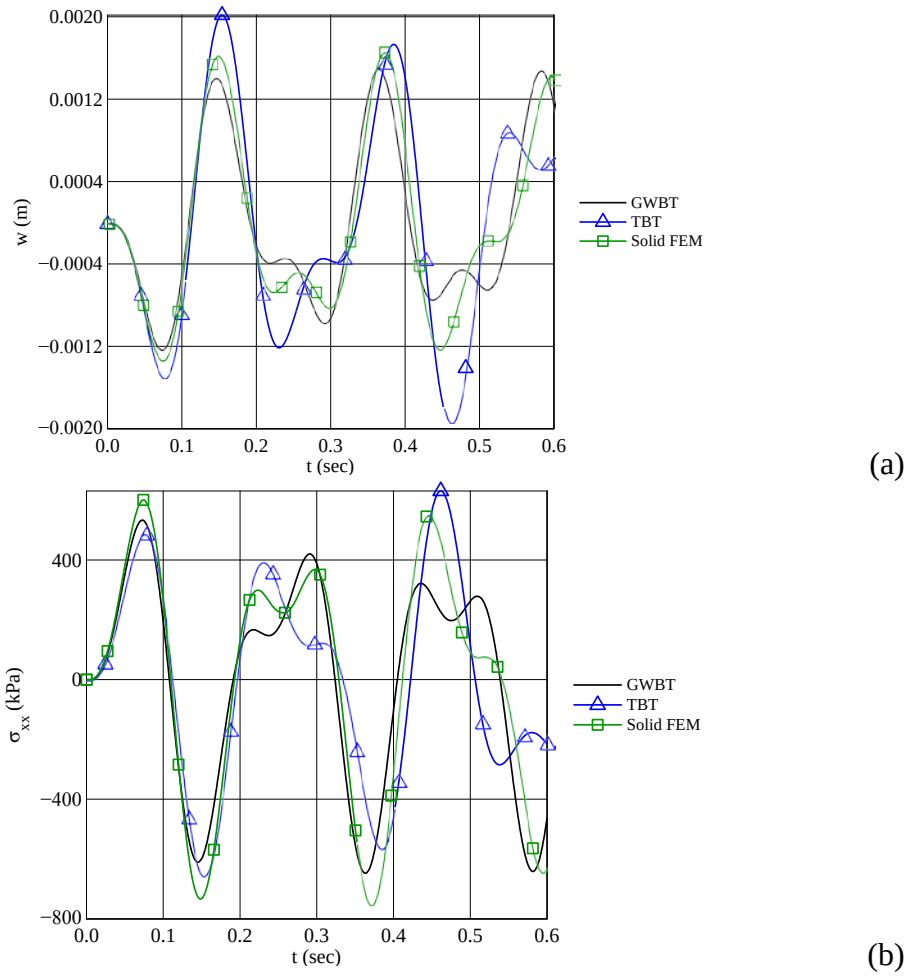

Fig. 10. Time history of the displacement w at $x = 16.94m$ (a) and normal stress σ_{xx} at the point A at $x = 1.5m$ (b) of the beam of example 2 for Load Case II.

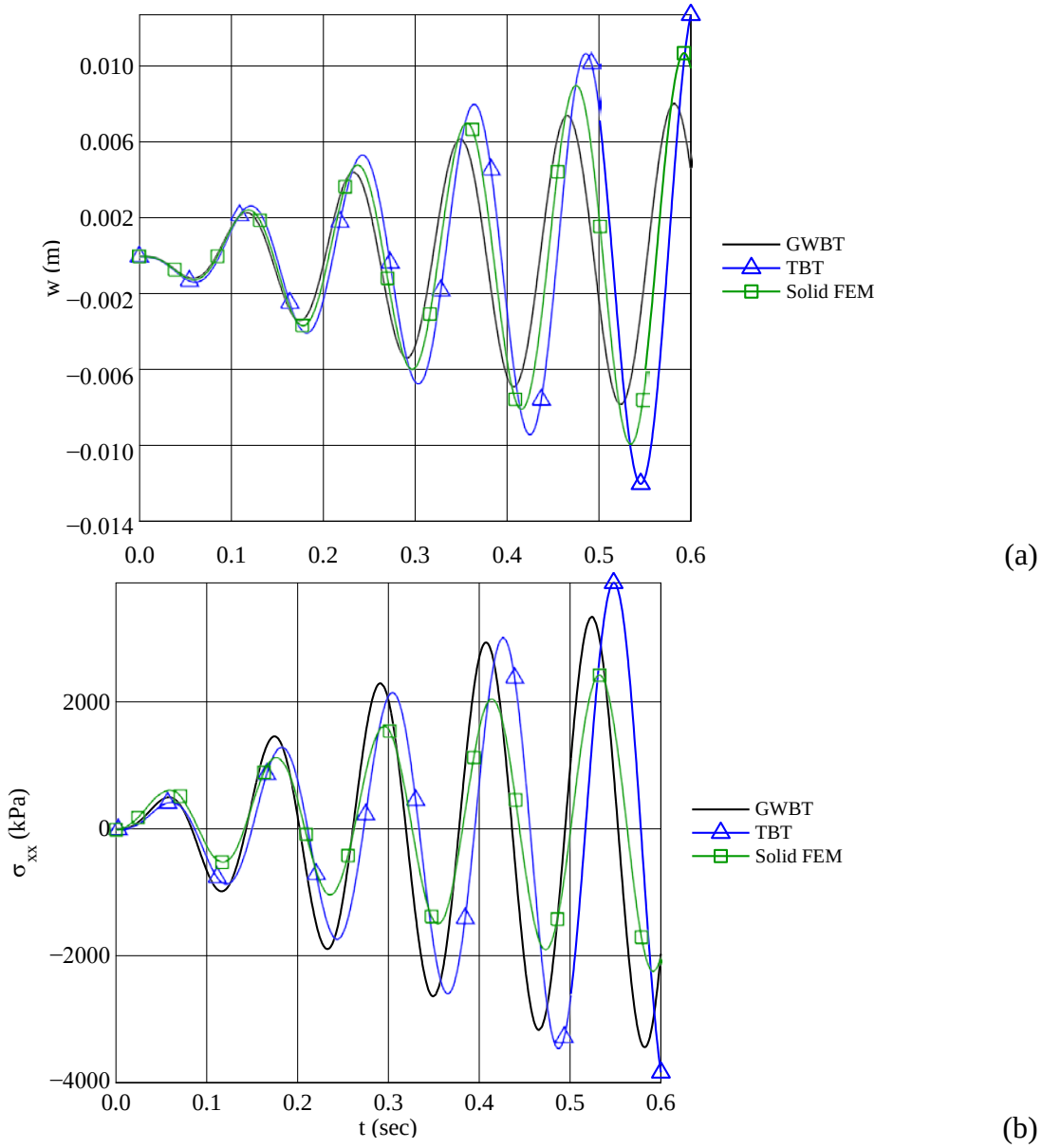

Fig. 11. Time history of the displacement w at $x = 16.94m$ (a) and normal stress σ_{xx} at the point A of the end 1 cross section (b) of the beam of example 2 for Load Case III.

as follows:

- The developed procedure retains most of the advantages of a BEM solution over a FEM approach, although it requires longitudinal domain discretization.
- The accuracy and the validity of the proposed method are noteworthy.
- TBT cannot predict the bending natural frequencies as accurate as GWBT can.
- By GWBT normal stresses are evaluated with high accuracy compared with solid FEM model results.
- The developed formulation is capable of giving accurate results without increasing the number of the involved kinematical unknowns.
- In the treated examples, the influence of flexural and torsional shear lag effects was apparent, modifying significantly the distribution of normal stress.

ACKNOWLEDGEMENTS

The third author would like to express her sincere thanks to the "Onassis Foundation" and the "A.G. Leventis Foundation" for the financial support she was given for her PhD studies during of which she participated in this research work.

REFERENCES

[1] Reissner, E. Analysis of shear lag in box beams by the principle of minimum potential energy. *Q. Appl. Math.*, 1946;41:268-78.

[2] Malcolm, D.J. and Redwood, R.G. Shear lag in stiffened box-girders. *J. Struct. Div. ASCE*, 1970;96(ST7):1403-15.

[3] Moffatt, K.R. and Dowling, P.J. Shear lag in steel box-girder bridges. *Struct. Engineer*, 1975;53:439-48.

[4] Razaqpur, A.G. and Li, H.G. A Finite Element with Exact Shape Functions for Shear Lag Analysis in Multi-Cell Box Girders. Computers & Structures, 1991;39(1):155-163.

[5] Dikaros, I.C. and Sapountzakis, E.J., Nonuniform Shear Warping Analysis of Composite Beams of Arbitrary Cross Section using the Boundary Element Method, Civil-Comp Press, Proceedings of the 14th International Conference on Civil, Structural and Environmental Engineering Computing, 2013.

[6] Eurocode 3: Design of Steel Structures – Part 1.5: Plated Structural Elements, European Committee for Standardization, prEN 1993-1-5: 2004.

[7] Eurocode 4: Design of Composite Steel and Concrete Structures – Part 1.1: General Rules and Rules for Buildings, European Committee for Standardization, prEN 1994-1-1: 2004.

[8] Eurocode 4: Design of Composite Steel and Concrete Structures – Part 2: General Rules and Rules for Bridges, European Committee for Standardization, prEN 1994-2: 2004.

[9] Ie, C.A. and Kosmatka, J.B. On the Analysis of Prismatic Beams Using First-Order Warping Functions. International Journal of Solids and Structures 1992;29(7):879-891.

[10] Vlasov, V., *Thin-walled elastic beams*. Israel Program for Scientific Translations, Jerusalem 1963.

[11] Sapountzakis, E.J. and Mokos, V.G. Warping Shear Stresses in Nonuniform Torsion of Composite Bars by BEM. Computational Methods in Applied Mechanics and Engineering 2003;192:4337-4353.

[12] Mokos, V.G. and Sapountzakis, E.J. Secondary Torsional Moment Deformation Effect by BEM. International Journal of Mechanical Sciences 2011;53, 897-909.

[13] Tsipiras, V.J. and Sapountzakis, E.J. Secondary Torsional Moment Deformation Effect in Inelastic Nonuniform Torsion of Bars of Doubly Symmetric Cross Section by BEM. International Journal of Non-linear Mechanics 2012;47, 68-84.

[14] El Fatmi, R. and Ghazouani, N. Higher Order Composite Beam Theory built on Saint-Venant's Solution. Part-I: Theoretical Developments. Composite Structures 2011;93:557-566.

[15] Tahan, N., Pavlović, M.N. and Kotsovos, M.D. Shear-Lag Revisited: The Use of Single Fourier Series for Determining the Effective Breadth in Plated Structures. Computers & Structures 1997;63(4):759-167.

[16] Katsikadelis, J.T. and Sapountzakis, E.J. A realistic estimation of the effective breadth of ribbed plates. International Journal of Solids and Structures 2002;39:897-910.

[17] Gupta, P.K., Singh, K.K. and Mishra, A. Parametric Study on Behaviour of Box-Girder Bridges Using Finite Element Method, Technical Note. Asian Journal of Civil Engineering (Building and Housing) 2010;11(1):135-148.

[18] Hjelmstad, K.D. Warping Effects in Transverse Bending of Thin-Walled Beams. Journal of Engineering Mechanics 1987;113(6):907-924.

[19] Ghazouani, N. and El Fatmi, R. Extension of the non-uniform warping theory to an orthotropic composite beam. Comptes Rendus Mecanique, 2010;338:704-711.

[20] Ghazouani, N. and El Fatmi, R. Higher Order Composite Beam Theory built on Saint-Venant's Solution. Part-II: Built-in Effects Influence on the Behavior of End-Loaded Cantilever Beams. Composite Structures 2011;93:567-581.

[21] Ferradi, M.K., Cespedes, X. and Arquie, M. A higher Order Beam Finite Element with Warping Eigenmodes. Engineering Structures 2013;46:748-762.

[22] Genoese, A., Genoese, A., Bilotta, A. and Garcea, G. A Mixed Beam Model with Non-Uniform Warpings Derived from the Saint Venànt Rod. Computers and Structures 2013;121:87-98.

[23] Jun, L., Rongying, S., Hongxing, H. and Xianding J. Response of monosymmetric thin-walled Timoshenko beams to random excitations. International Journal of Solids and Structures 2004; 41:6023-6040.

[24] Kim, N.I., Seo, K. J. and Kim, M. Y. Free vibration and spatial stability of non-symmetric thin-walled curved beams with variable curvatures. International Journal of Solids and Structures 2003; 40:3107-3128.

[25] Kim, N.I., Shin, D.K. and Park, Y.S. Dynamic stiffness matrix of thin-walled composite I-beam with symmetric and arbitrary laminations. Journal of Sound and Vibration 2008; 318:364-388.

[26] Kwak, H.G., Kim, D.Y. and Lee, H.W. Effect of warping in geometric nonlinear analysis of spatial beams. Journal of Constructional Steel Research 2001; 57:729-751.

[27] Librescu, L., Qin, Z. and Ambur, D.R. Implications of warping restraint on statics and dynamics of elastically tailored thin-walled composite beams. International Journal of Mechanical Sciences 2003; 45:1247-1267.

[28] Mitra, M., Gopalakrishnan, S. and Bhat, M. S. A new super convergent thin walled composite beam element for analysis of box beam structures. International Journal of Solids and Structures 2004; 41:1491-1518.

[29] Piovan, M.T. and Cortidnez, V.H. Out-of-plane vibrations of shear deformable continuous horizontally curved thin-walled beams 2000; 237(1):101-118.

[30] Piovan, M. T. and Cortınez, V.H. Mechanics of shear deformable thin-walled beams made of composite materials. Thin-Walled Structures 2007; 45:37-6

[31] Senjanovic, I., Catipovic, I., and Tomasevic, S. Coupled flexural and torsional vibrations of ship-like girders. Thin-Walled Structures 2007; 45:1002-1021.

[32] Piovan, M.T. and Cortınez, V.H.. Mechanics of thin-walled curved beams made of composite materials, allowing for shear deformability. Thin-Walled Structures 2007 45:759-789.

[33] A. Prokic. On triply coupled vibrations of thin-walled beams with arbitrary cross-section Journal of Sound and Vibration 2005; 279:723-737.

[34] Shadmehri, F., Haddadpour, H. and Kouchakzadeh M.A. Flexural–torsional behavior of thin-walled composite beams with closed cross-section. Thin-Walled Structures 2007; 45:699-705.

[35] Piovan, M.T., Filipich, C.P. and Cortınez, V.H. Exact solutions for coupled free vibrations of tapered shear-flexible thin-walled composite beams. Journal of Sound and Vibration 2008; 316:298-316.

[36] Le, T.N., Battini, J.M. and Hjiaj, M. Corotational formulation for nonlinear dynamics of beams with arbitrary thin-walled open cross-sections. Computers and Structures 2014; 134:112-127.

[37] Egidio, A.D., Luongo, A. and Vestroni, F. A non-linear model for the dynamics of open cross-section thin-walled beams-Part I: formulation International Journal of Non-Linear Mechanics 2003; 38:1067-1081.

[38] Minghini, F., Tullini, N. and Laudiero, F. Vibration analysis with second-order effects of pultruded FRP frames using locking-free elements Thin-Walled Structures 2009; 47:136-150.

[39] Sapountzakis, E.J. and Mokos, V.G. Vibration analysis of 3-D composite beam elements including warping and shear deformation effects Journal of Sound and Vibration 2007; 306:818-834.

[40] Sapountzakis, E.J. and Tsipiras, V.J. Nonlinear nonuniform torsional vibrations of bars by the boundary element method Journal of Sound and Vibration 2010; 329:1853-1874.

[41] Sapountzakis, E.J. and , Dikaros, I.C. Non-linear flexural–torsional dynamic analysis of beams of arbitrary cross section by BEM International Journal of Non-Linear Mechanics 2011; 46:782-794.

[42] Stoykov, S. and Ribeiro, P. Nonlinear forced vibrations and static deformations of 3D beams with rectangular cross section: The influence of warping, shear deformation and longitudinal displacements International Journal of Mechanical Sciences 2010; 52:1505-1521.

[43] Stoykov, S.and Ribeiro, P. Non-linear vibrations of beams with non-symmetrical cross sections International Journal of Non-Linear Mechanics 2013; 55:153-169.

[44] Voros, G.M. Buckling and free vibration analysis of stiffened panels Thin-Walled Structures 2009; 47:382-390.

[45] Yu, A.M., Yang, C.J., Nie, G.H. Analytical formulation and evaluation for free vibration of naturally curved and twisted beams Journal of Sound and Vibration 2010; 329:1376-1389.

[46] Sapountzakis, E.J. and Mokos, V.G. Dynamic analysis of 3-D beam elements including warping and shear deformation effects International Journal of Solids and Structures 2006; 43:6707-6726.

[47] Sapountzakis, E.J., Tsipiras, V.J. Warping shear stresses in nonlinear nonuniform torsional vibrations of bars by BEM Engineering Structures 2010; 32:741-752.

[48] Li, P., Gantoi, F.M. and Shabana, A.A. Higher order representation of the beam cross section deformation in large displacement finite element analysis Journal of Sound and Vibration 2011; 330:6495-6508.

[49] Dikaros, I.C. and Sapountzakis, E.J. Generalized Warping Analysis of Composite Beams of an Arbitrary Cross Section by BEM. I: Theoretical Considerations and Numerical Implementation. Journal of Engineering Mechanics 2014; 140(9): 04014062.

[50] Dikaros, I.C. and Sapountzakis, E.J. Generalized Warping Analysis of Composite Beams of an Arbitrary Cross Section by BEM. II: Numerical Applications. Journal of Engineering Mechanics 2014; 140(9): 04014063.

[51] Siemens PLM Software Inc., NX Nastran User's Guide; 2008.

[52] Katsikadelis, J.T. The Analog Equation Method. A Boundary – only Integral Equation Method for Nonlinear Static and Dynamic Problems in General Bodies. Theoretical and Applied Mechanics 2002;27:13-38.

[53] Sapountzakis, E.J. and Katsikadelis, J.T. Analysis of plates reinforced with beams. Computational Mechanics 2000;26:66-74.

[54] Katsikadelis, J.T. Boundary Elements: Theory and Applications, Elsevier, Amsterdam-London; 2002.

[55] Beer, G., Smith, I. and Duenser, Ch. The Boundary Element Method with Programming – For Engineers and Scentists, Springer Wien Niew York; 2008.

[56] Chopra, A.K. Dynamics of Structures Theory and Applications to Earthquake Engineering, Prentice Hall, Upper Saddle River, NJ, 1995.